

Unified EOS and pasta phases for neutron stars

Hong Shen *Nankai University, Tianjin, China*

申虹 南開大学 天津 中国

Collaborators:

Jinniu Hu *Nankai University, Tianjin, China*

Shishao Bao *Shanxi Normal University, China*

Xuhao Wu *Nankai University, Tianjin, China*

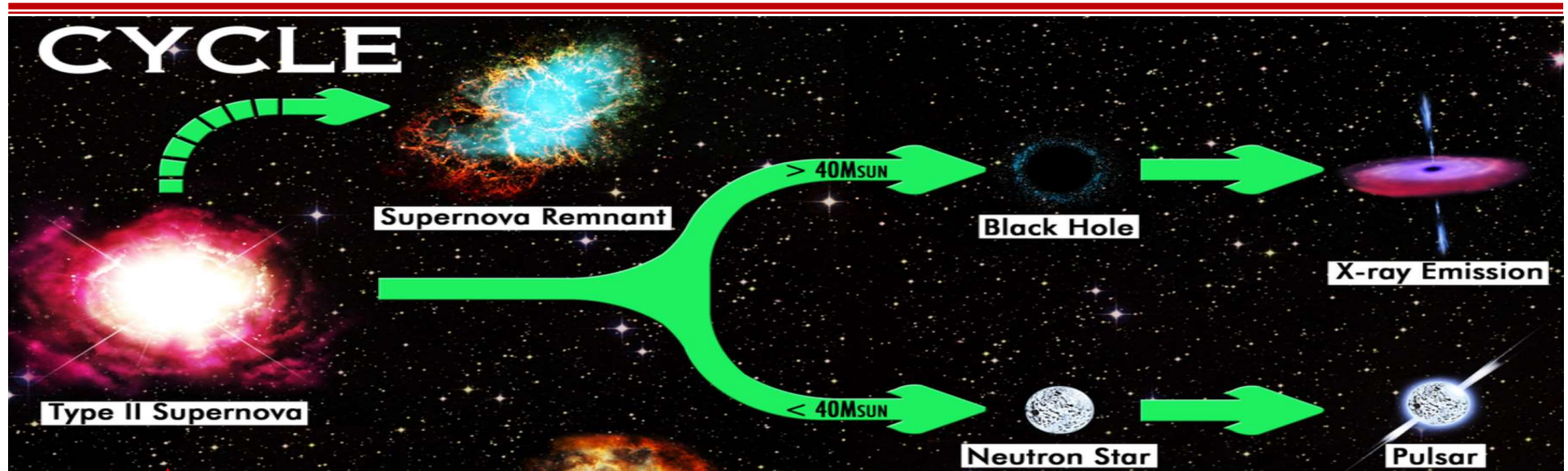
Fan Ji *Nankai University, Tianjin, China*



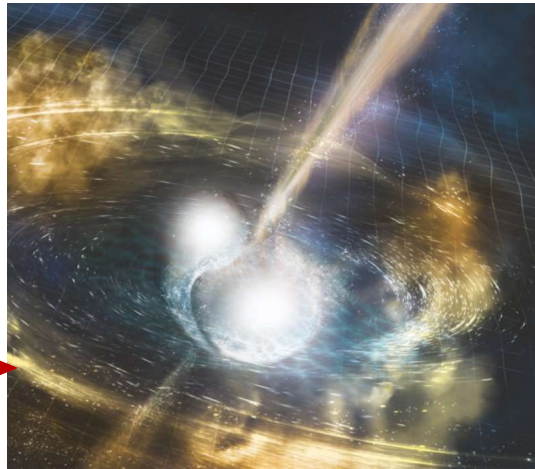
Contents

- Introduction
- Unified EOS for neutron stars
- Nuclear pasta phases
- Hadron-quark pasta phases
- New EOS table for supernovae
- Summary

Introduction



Equation of State (EOS)



binary neutron star merger

Classification of EOS

EOS for supernovae

temperature (T):

0 ~ 100 MeV

proton fraction (Y_p):

0 ~ 0.6

construction:

nonuniform + uniform

EOS for neutron stars

temperature (T):

T = 0

proton fraction (Y_p):

β equilibrium

construction:

crusts + core

EOS for supernovae

single nucleus approximation (SNA)

J. M. Lattimer and F. D. Swesty, Nucl. Phys. A 535, 331 (1991)

liquid-drop model with Skyrme force

H. Shen, H. Toki, K. Oyamatsu, K. Sumiyoshi, Prog. Theor. Phys. 100, 1013 (1998)

H. Shen, H. Toki, K. Oyamatsu, K. Sumiyoshi, Astrophys. J. Suppl. 197, 20 (2011)

Thomas-Fermi with RMF (TM1)

H. Togashi, K. Nakazato, Y. Takehara, S. Yamamuro, H. Suzuki, M. Takano, NPA 961 (2017) 78

Thomas-Fermi with realistic nuclear forces

nuclear statistical equilibrium (NSE)

M. Hempel and J. Schaffner-Bielich, Nucl. Phys. A 837, 210 (2010)

A.S. Botvina, I.N. Mishustin, Nucl. Phys. A 843, 98 (2010)

S. Furusawa, K. Sumiyoshi, S. Yamada, H. Suzuki, Astrophys. J. 772, 95 (2013)

S. Typel, G. Ropke, T. Klahn, D. Blaschke, H. Wolter, Phys. Rev. C 81, 015803 (2010)

G. Shen, C. J. Horowitz, E. O'Connor, Phys. Rev. C 83, 065808 (2011)

⋮

EOS for neutron stars

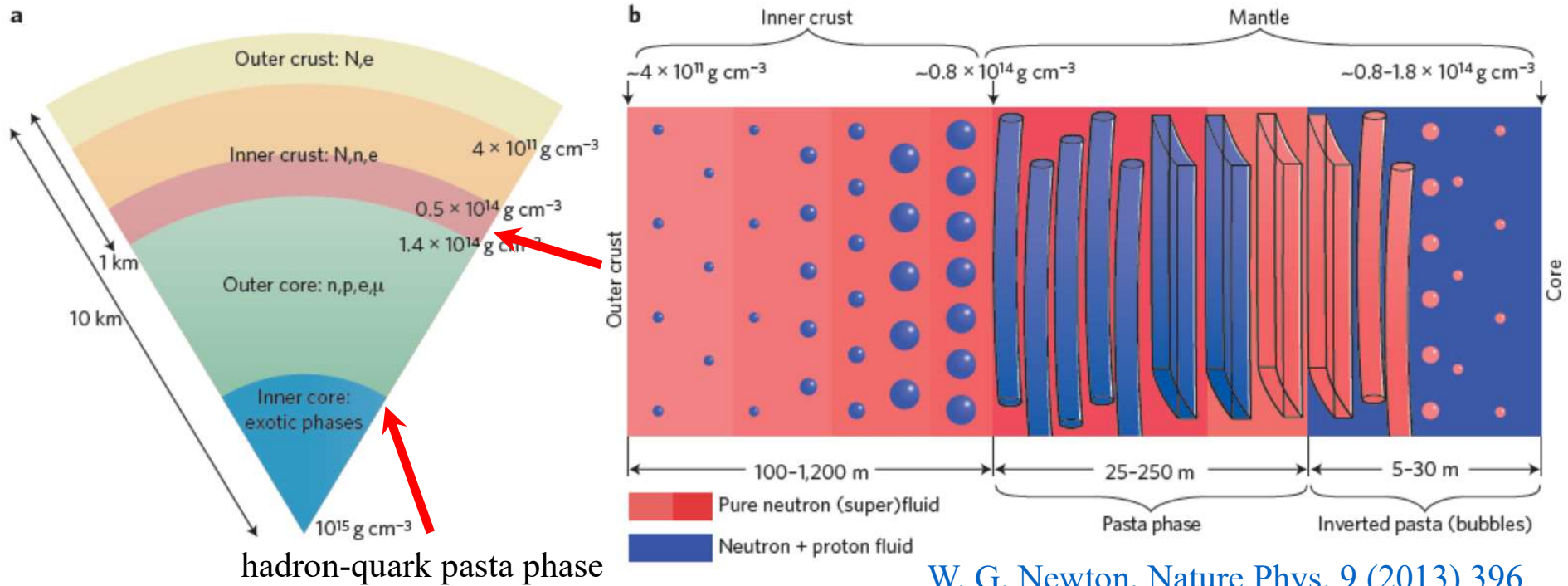
$$T = 0, \quad \rho \sim 10^7 - 10^{15} \text{ g/cm}^3$$

outer crust $e+A \rightarrow e+n+A$

inner crust $e+n+A$

liquid core $(e, \mu) + (n, p)$

+ hyperons
quarks
:



W. G. Newton, Nature Phys. 9 (2013) 396

works by Heiselberg, Maruyama, Tatsumi, Endo, Yasutake, Weber, ...

EOS for neutron stars

unified EOS: crusts + core (consistent)

F. Douchin and P. Haensel, AA 380, 151 (2001)

liquid-drop model with Skyrme force

F. Fantina, N. Chamel, J. M. Pearson, and S. Goriely, AA 559, A128 (2013)

B. K. Sharma, M. Centelles, X. Vinas, M. Baldo, G. F. Burgio, AA 584, A103 (2015)

Thomas-Fermi with nonrelativistic nuclear models

H. Shen, PRC 65, 035802 (2002)

T. Miyatsu, S. Yamamuro, K. Nakazato, ApJ 777, 4 (2013)

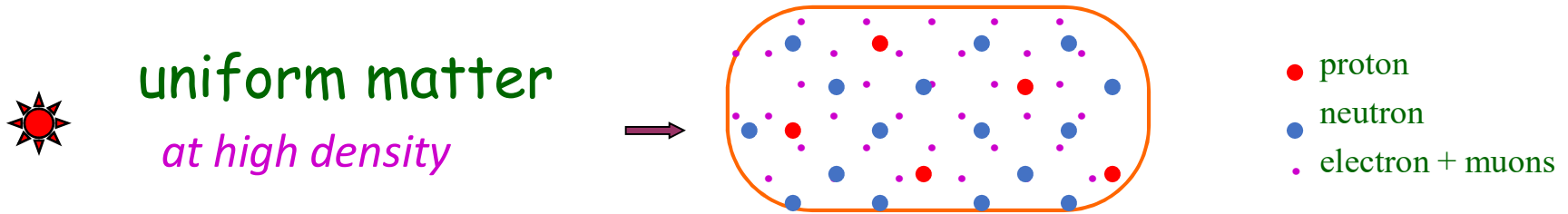
M. Fortin, C. Providencia, Ad. R. Raduta et al., PRC 94, 035804 (2016)

Thomas-Fermi with relativistic nuclear models

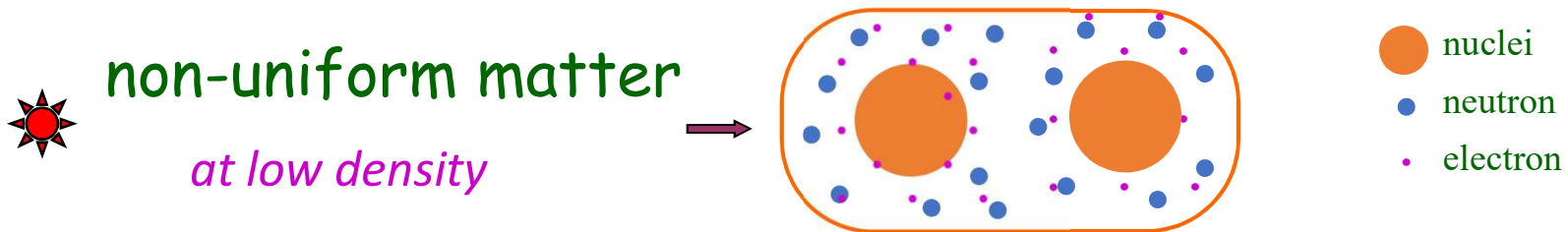
nonunified EOS: crusts + core (inconsistent)

BBP EOS }
NV EOS } + core EOS
DH EOS }

Models used for EOS



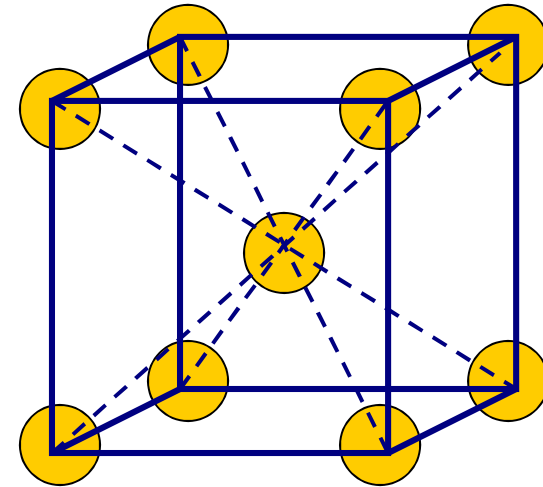
RMF (relativistic Mean Field)



RMF + Thomas-Fermi approximation

Thomas-Fermi approximation

- * body-centered cubic lattice
- * Wigner-Seitz approximation
- * RMF input



$$E = E_{bulk} + E_{surface} + E_{Coulomb} + E_{Lattice} + E_{electron}$$



RMF model

- * generated RMF models with different L by turning g_ρ and Λ_v

$$\begin{aligned}
 \mathcal{L}_{\text{RMF}} = & \bar{\psi} \left[i\gamma_\mu \partial^\mu - (M + g_\sigma \sigma) - \left(g_\omega \omega^\mu + \frac{g_\rho}{2} \tau_a \rho^{a\mu} \right) \gamma_\mu \right] \psi \\
 & + \frac{1}{2} \partial_\mu \sigma \partial^\mu \sigma - \frac{1}{2} m_\sigma^2 \sigma^2 - \frac{1}{3} g_2 \sigma^3 - \frac{1}{4} g_3 \sigma^4 \\
 & - \frac{1}{4} W_{\mu\nu} W^{\mu\nu} + \frac{1}{2} m_\omega^2 \omega_\mu \omega^\mu + \frac{1}{4} c_3 (\omega_\mu \omega^\mu)^2 \\
 & - \frac{1}{4} R_{\mu\nu}^a R^{a\mu\nu} + \frac{1}{2} m_\rho^2 \rho_\mu^a \rho^{a\mu} + \Lambda_v \left(g_\omega^2 \omega_\mu \omega^\mu \right) \left(g_\rho^2 \rho_\mu^a \rho^{a\mu} \right)
 \end{aligned}$$

- * all models have the same isoscalar saturation properties

TABLE II. Parameters g_ρ and Λ_v generated from the TM1 model for different slope L at saturation density n_0 with fixed symmetry energy $E_{\text{sym}} = 28.05$ MeV at $n_{\text{fix}} = 0.11 \text{ fm}^{-3}$. The last two lines show the symmetry energy at saturation density, $E_{\text{sym}}(n_0)$, and the neutron-skin thickness of ^{208}Pb , Δr_{np} . The original TM1 model has $L = 110.8$ MeV.

L (MeV)	40.0	50.0	60.0	70.0	80.0	90.0	100.0	110.8
g_ρ	13.9714	12.2413	11.2610	10.6142	10.1484	9.7933	9.5114	9.2644
Λ_v	0.0429	0.0327	0.0248	0.0182	0.0128	0.0080	0.0039	0.0000
$E_{\text{sym}}(n_0)$ (MeV)	31.38	32.39	33.29	34.11	34.86	35.56	36.22	36.89
Δr_{np} (fm)	0.1574	0.1886	0.2103	0.2268	0.2402	0.2514	0.2609	0.2699

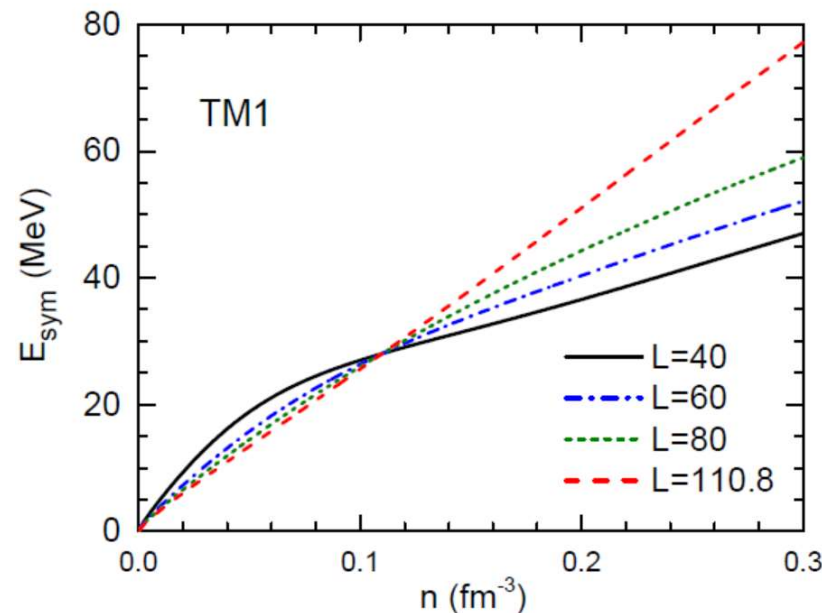
Symmetry energy effects

- * energy per particle w as function of n and $\alpha = \frac{n_n - n_p}{n}$

$$w = w_0 + \frac{K_0}{18n_0^2}(n - n_0)^2 + \left[S_0 + \frac{L}{3n_0}(n - n_0) \right] \alpha^2$$

symmetry energy slope

$$L = 3n_0 \left[\frac{\partial E_{\text{sym}}(n_b)}{\partial n_b} \right]_{n_b=n_0}$$



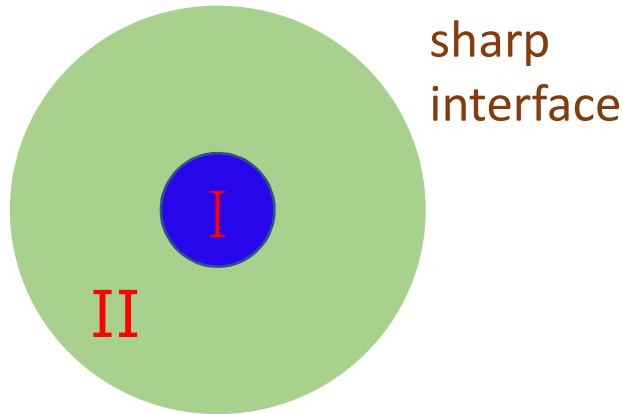
Nuclear pasta phases

crust-core transition

- * **spinodal instability** (no surface and Coulomb)
determined by the curvature of the free energy
- * **bulk calculation** (no surface and Coulomb)
phase equilibrium determined by the Gibbs conditions
- * **coexisting phases (CP)** (surface and Coulomb perturbatively)
phase equilibrium determined by the Gibbs conditions
- * **compressible liquid-drop (CLD)** (minimization of free energy)
phase equilibrium determined by minimization
- * **Thomas-Fermi (TF)** (realistic description)

Methods for pasta phases

Coexisting phases (CP)



Gibbs equilibrium

$$P^I = P^{II}$$

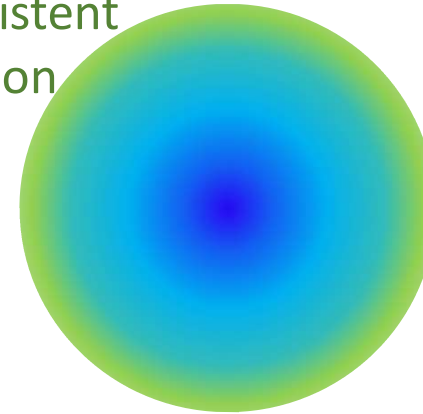
$$\mu_i^I = \mu_i^{II}$$

perturbatively

Coulomb and surface energies

Thomas-Fermi (TF)

self-consistent distribution



$$-\nabla^2 \sigma + m_\sigma^2 \sigma + g_2 \sigma^2 + g_3 \sigma^3 = -g_\sigma (n_p^s + n_n^s),$$

$$-\nabla^2 \omega + m_\omega^2 \omega + c_3 \omega^3 + 2\Lambda_v g_\omega^2 g_\rho^2 \rho^2 \omega = g_\omega (n_p + n_n)$$

$$-\nabla^2 \rho + m_\rho^2 \rho + 2\Lambda_v g_\omega^2 g_\rho^2 \omega^2 \rho = \frac{g_\rho}{2} (n_p - n_n),$$

$$-\nabla^2 A = e (n_p - n_e),$$

self-consistently

Symmetry energy \leftrightarrow pasta phases, crust-core

K. Oyamatsu, K. Iida, Phys. Rev. C 75, 015801 (2007)

B. A. Li, L. W. Chen, C. M. Ko, Phys. Rep. 464, 113 (2008)

F. Grill, C. Providência, S. S. Avancini, Phys. Rev. C 85, 055808 (2012)

Z. Zhang, L. W. Chen, Phys. Lett. B 726, 234 (2013)

S. S. Bao, H. Shen, Phys. Rev. C 89, 045807 (2014)

S. S. Bao, J. N. Hu, Z. W. Zhang, H. Shen, Phys. Rev. C 90, 045802 (2014)

S. S. Bao, H. Shen, Phys. Rev. C 91, 015807 (2015)

adjust g_ρ
 Λ_V

fix symmetry energy at 0.11 fm^{-3}
different symmetry energy slope L

saturation property
neutron star mass $\sim 2 M_\odot$
finite nuclei

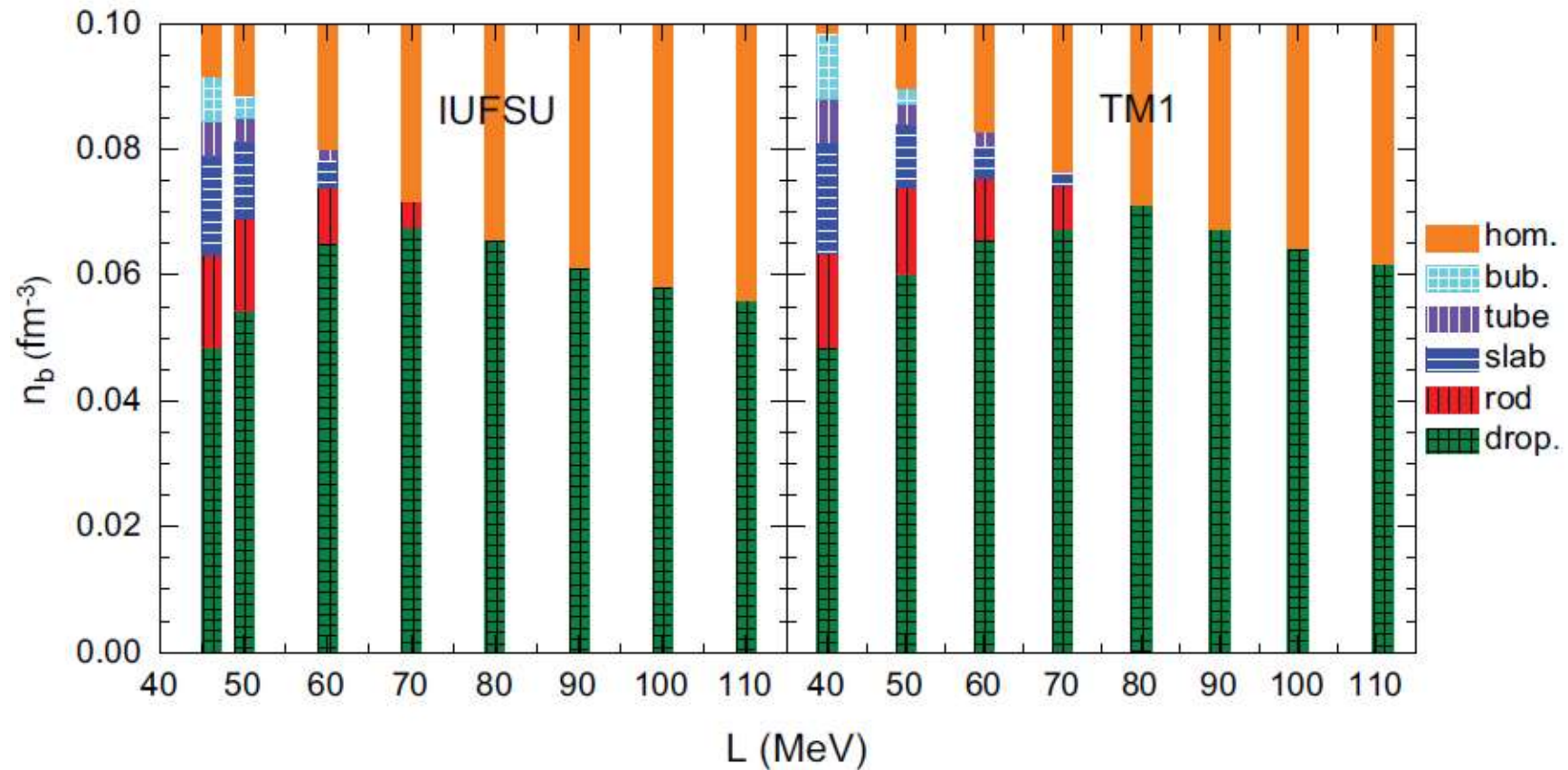
TM1 set \rightarrow

L (MeV)	40.0	50.0	60.0	70.0	80.0	90.0	100.0	110.8
g_ρ	13.9714	12.2413	11.2610	10.6142	10.1484	9.7933	9.5114	9.2644
Λ_V	0.0429	0.0327	0.0248	0.0182	0.0128	0.0080	0.0039	0.0000

IUFSU set \rightarrow

L (MeV)	47.2	50.0	60.0	70.0	80.0	90.0	100.0	110.0
g_ρ	13.5900	12.8202	11.1893	10.3150	9.7537	9.3559	9.0558	8.8192
Λ_V	0.0460	0.0420	0.0305	0.0220	0.0153	0.0098	0.0051	0.0011

Phase diagram of inner crust (TF)

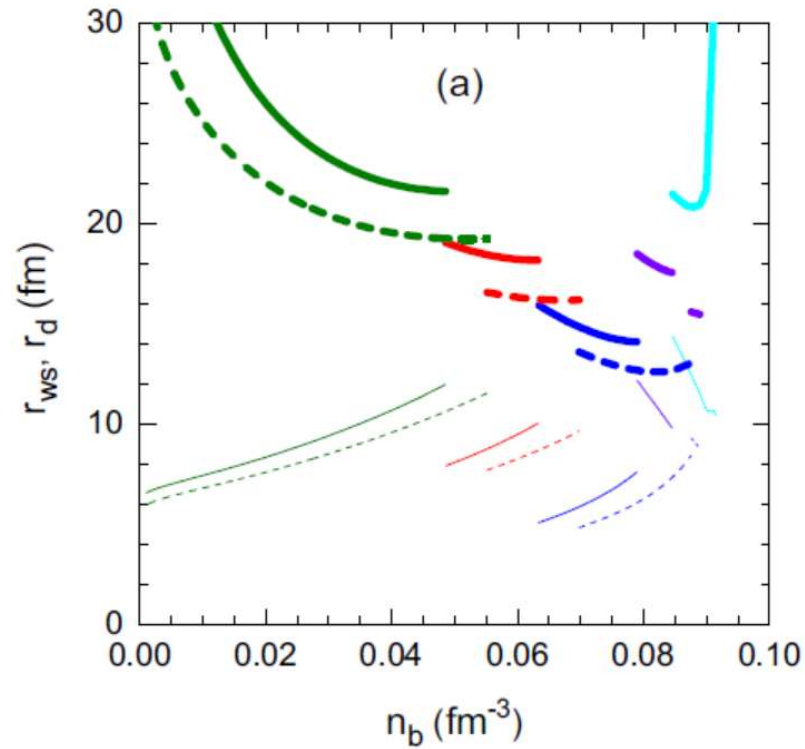


S. S. Bao, H. Shen, Phys. Rev. C 91, 015807 (2015)

smaller L corresponds to more pasta phases

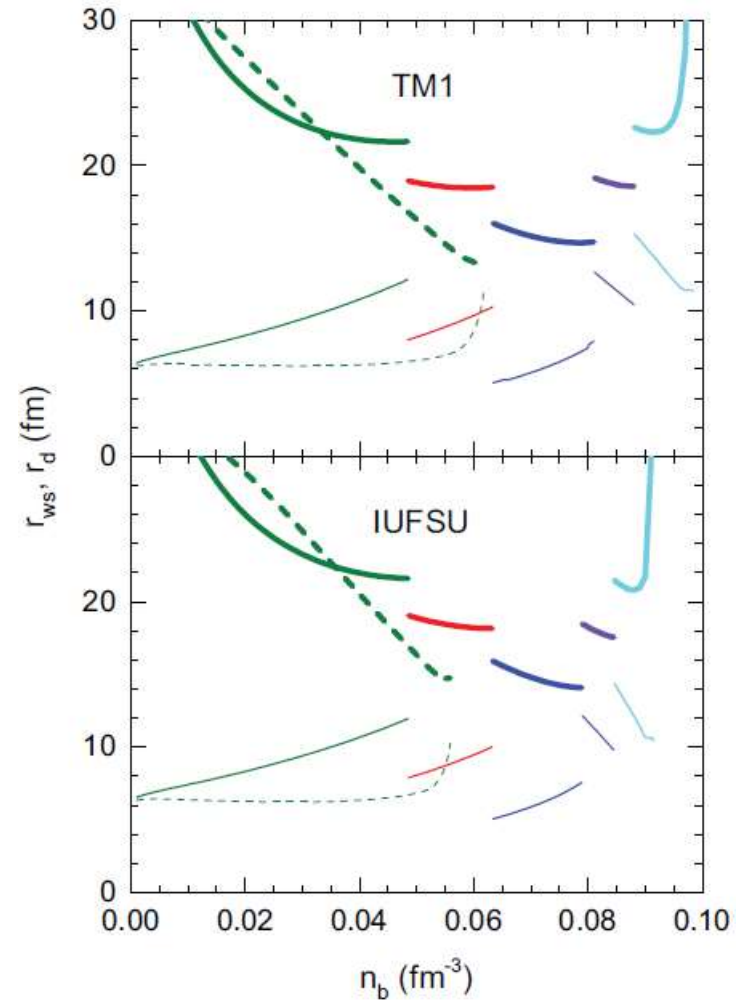
smaller L corresponds to larger crust-core transition density

Pasta phase properties



size of Wigner-Seitz cell
size of pasta structure

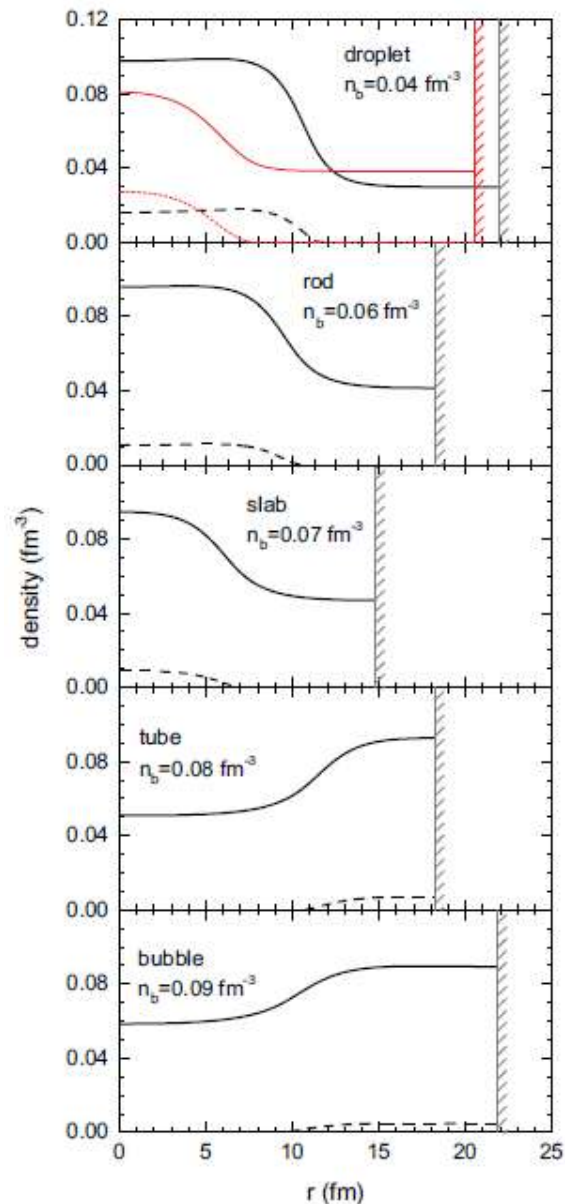
TF (solid lines) & CP (dashed lines)



small L (solid lines)

large L (dashed lines)

Distributions of neutrons and protons



— neutron
- - - proton

L=110 MeV

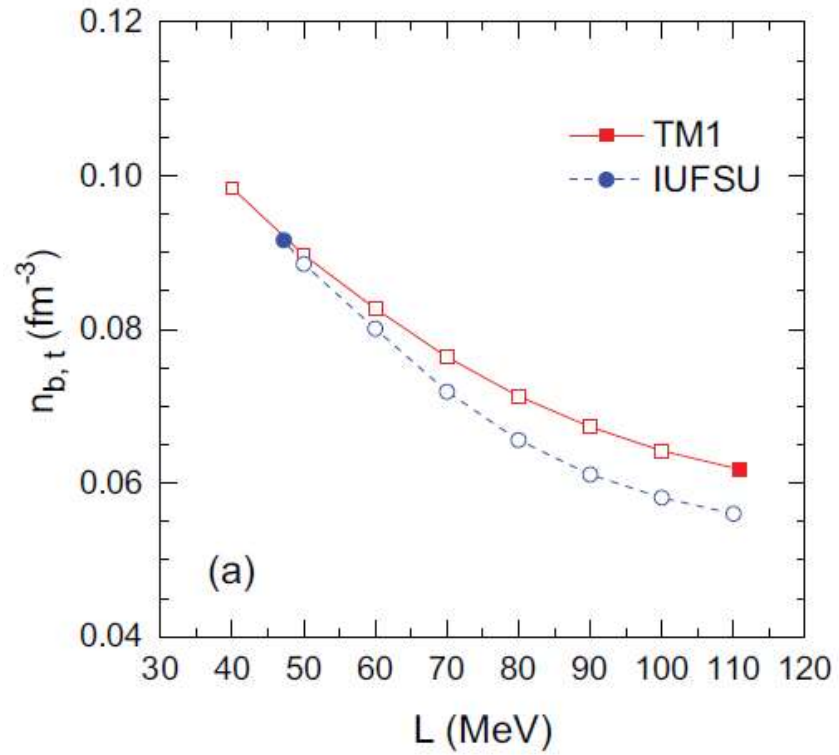
— neutron
- - - proton

L=47.2 MeV

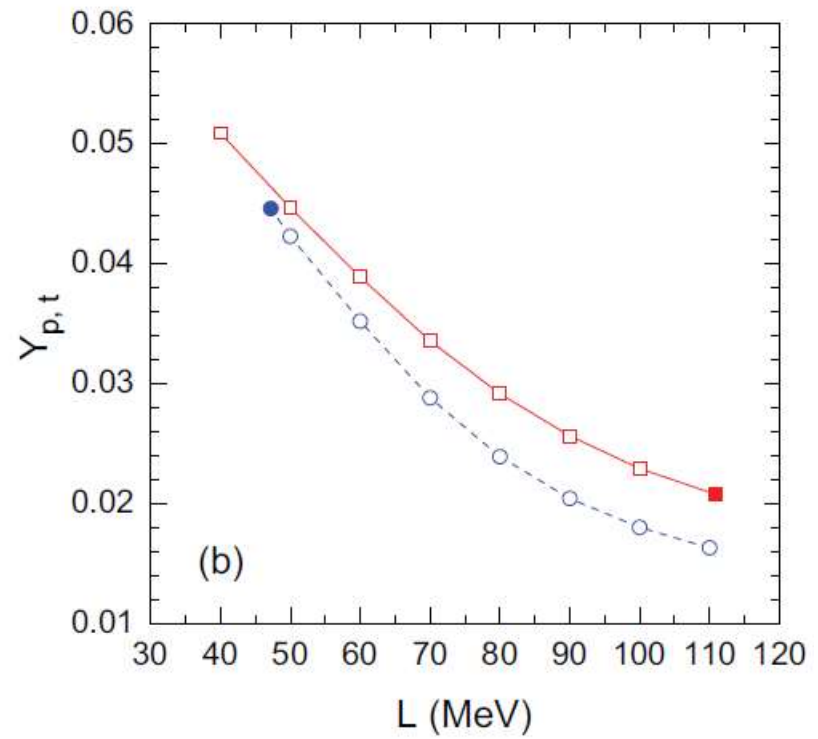
self-consistent Thomas-Fermi
with the IUFSU model

S. S. Bao, H. Shen, Phys. Rev. C 91, 015807 (2015)

Crust-core transition

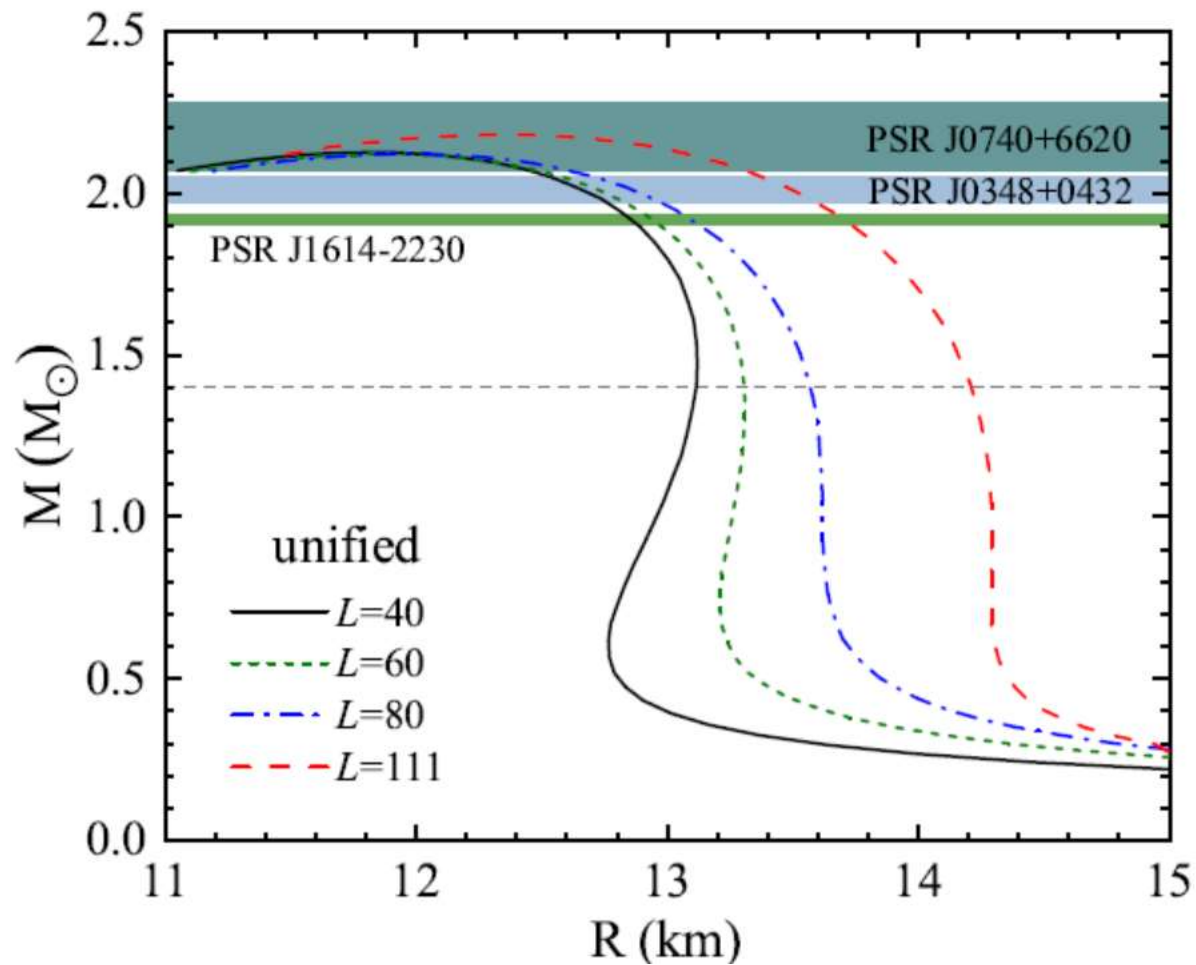


transition density



proton fraction

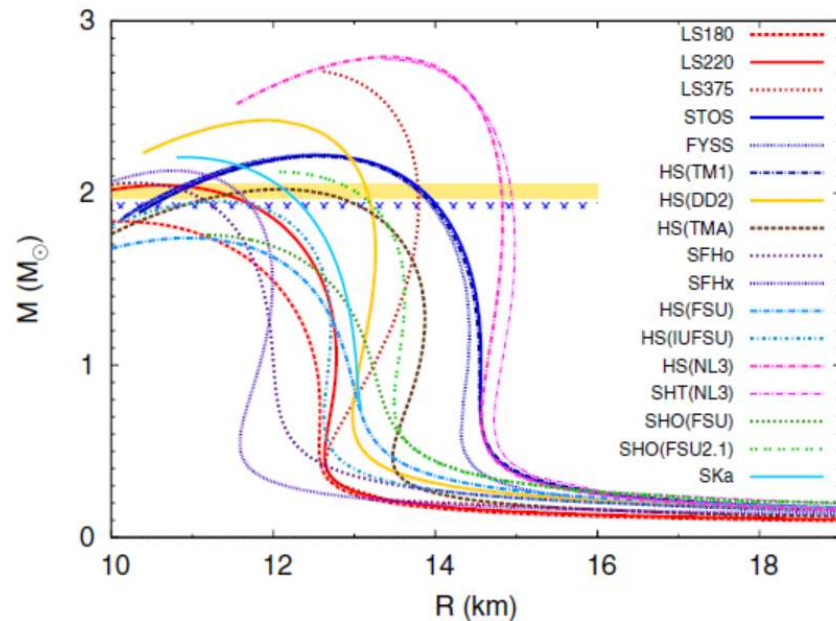
Neutron stars with unified EOS



F. Ji, S. S. Bao, J. N. Hu, H. Shen, to appear in PRC

smaller L corresponds to smaller R

symmetry energy and neutron stars

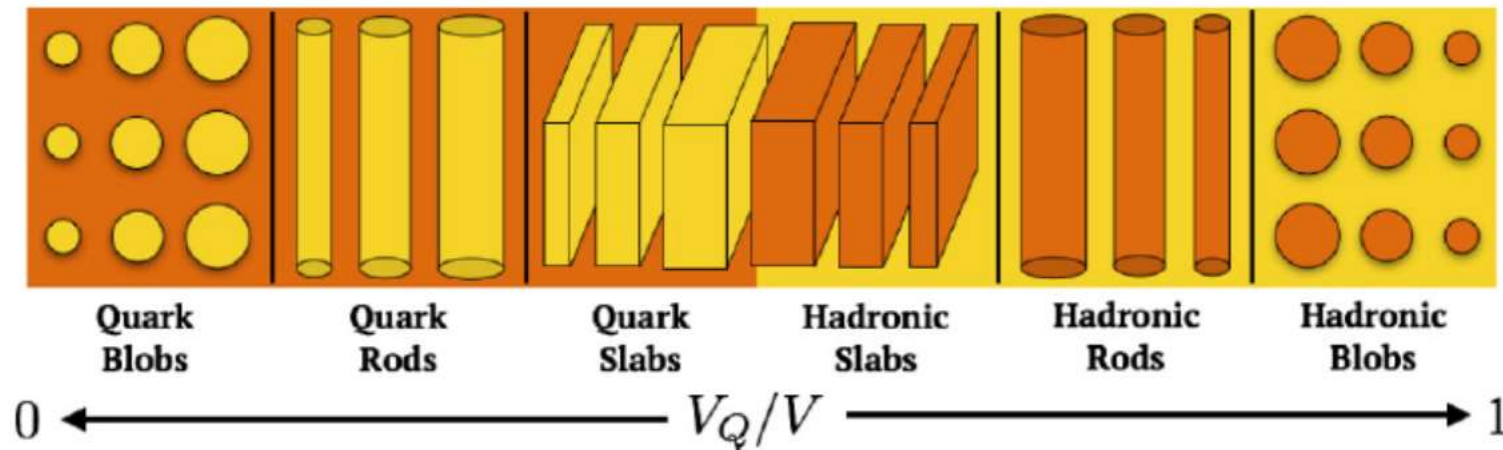


Nuclear interaction	n_{sat} (fm $^{-3}$)	B_{sat} (MeV)	K (MeV)	Q (MeV)	J (MeV)	L (MeV)
SKa	0.155	16.0	263	-300	32.9	74.6
LS180	0.155	16.0	180	-451	28.6 ^a	73.8
LS220	0.155	16.0	220	-411	28.6 ^a	73.8
LS375	0.155	16.0	375	176	28.6 ^a	73.8
TM1	0.145	16.3	281	-285	36.9	110.8
TMA	0.147	16.0	318	-572	30.7	90.1
NL3	0.148	16.2	272	203	37.3	118.2
FSUgold	0.148	16.3	230	-524	32.6	60.5
FSUgold2.1	0.148	16.3	230	-524	32.6	60.5
IUFSU	0.155	16.4	231	-290	31.3	47.2
DD2	0.149	16.0	243	169	31.7	55.0
SFHo	0.158	16.2	245	-468	31.6	47.1
SFHx	0.160	16.2	239	-457	28.7	23.2

M. Oertel, M. Hempel, T. Klöhn, S. Typel, Rev. Mod. Phys. 89, 015007 (2017)

smaller L corresponds to smaller R

Hadron-quark psata phases



W. M. Spinella, F. Weber, G. A. Contrera, M. G. Orsaria, EPJA 52 (2016) 61

hadronic phase

+

quark phase

Brueckner-Hartree-Fock

Relativistic mean-field

chiral effective field

:

MIT bag model

2-flavor NJL model

3-flavor NJL model

:

Hadron-quark psata phases

NJL model

$$\begin{aligned}\mathcal{L}_{\text{NJL}} = & \bar{q} (i\gamma_\mu \partial^\mu - m^0) q \\ & + G_S \sum_{a=0}^8 \left[(\bar{q} \lambda_a q)^2 + (\bar{q} i\gamma_5 \lambda_a q)^2 \right] \\ & - K \left\{ \det [\bar{q} (1 + \gamma_5) q] + \det [\bar{q} (1 - \gamma_5) q] \right\} \\ & - \underline{G_V} \sum_{a=0}^8 \left[(\bar{q} \gamma^\mu \lambda_a q)^2 + (\bar{q} \gamma^\mu \gamma_5 \lambda_a q)^2 \right],\end{aligned}$$

Gap equation

$$m_i^* = m_i^0 - 4G_S \langle \bar{q}_i q_i \rangle + 2K \langle \bar{q}_j q_j \rangle \langle \bar{q}_k q_k \rangle$$

Hadron-quark pasta phases

hadron-quark mixed phase

$$\varepsilon_{\text{MP}} = u\varepsilon_{\text{QP}} + (1 - u)\varepsilon_{\text{HP}} + \varepsilon_{\text{surf}} + \varepsilon_{\text{Coul}}$$

$$\varepsilon_{\text{surf}} = \frac{D\sigma u_{\text{in}}}{r_D},$$
$$\varepsilon_{\text{Coul}} = \frac{e^2}{2} (\delta n_c)^2 r_D^2 u_{\text{in}} \Phi(u_{\text{in}})$$

$$\Phi(u_{\text{in}}) = \begin{cases} \frac{1}{D+2} \left(\frac{2 - Du_{\text{in}}^{1-2/D}}{D-2} + u_{\text{in}} \right), & D = 1, 3, \\ \frac{u_{\text{in}} - 1 - \ln u_{\text{in}}}{D+2}, & D = 2. \end{cases}$$

Hadron-quark pasta phases

- * **Gibbs construction** (no surface and Coulomb)

surface tension: $\sigma = 0 \rightarrow \varepsilon_{\text{surf}} = 2\varepsilon_{\text{Coul}} = 0$

$$P_{\text{HP}} = P_{\text{QP}}, \quad \mu_n = \mu_u + 2\mu_d, \quad \mu_e^{\text{HP}} = \mu_e^{\text{QP}}$$

- * **Maxwell construction** (no surface and Coulomb)

surface tension: large $\sigma \rightarrow$ local charge neutrality $\rightarrow \varepsilon_{\text{surf}} = 2\varepsilon_{\text{Coul}} = 0$

$$P_{\text{HP}} = P_{\text{QP}}, \quad \mu_n = \mu_u + 2\mu_d, \quad \mu_e^{\text{HP}} \neq \mu_e^{\text{QP}}$$

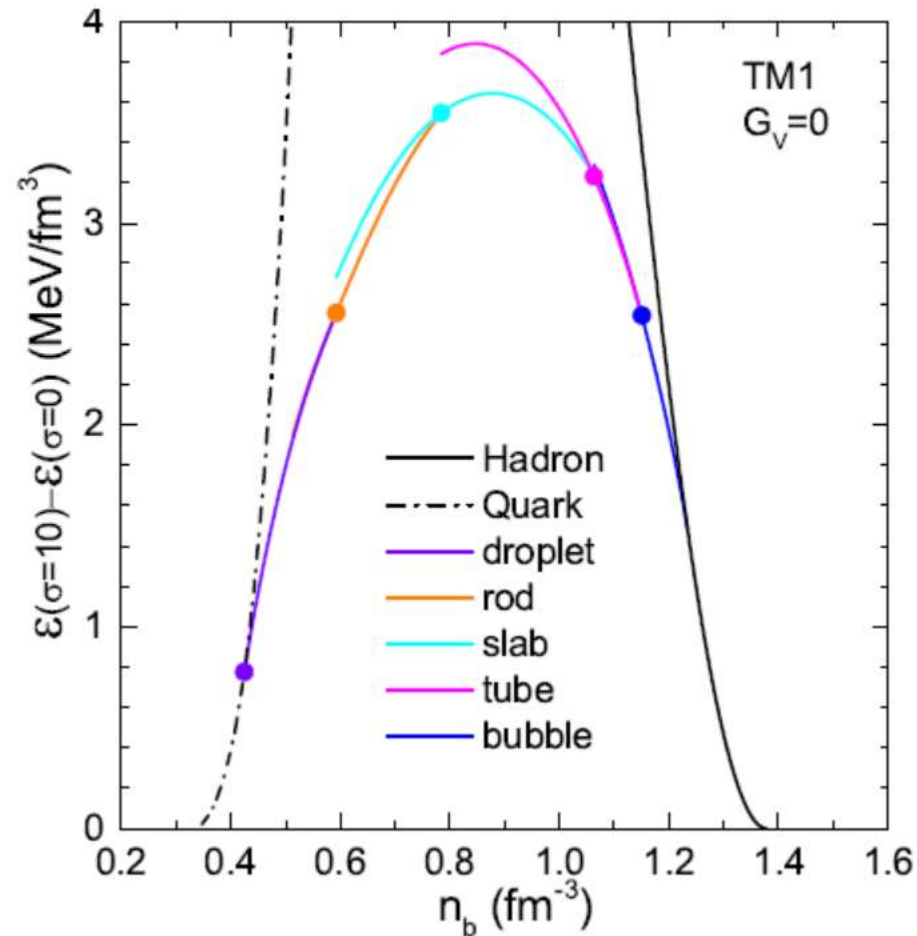
- * **coexisting phases (CP)** (surface and Coulomb perturbatively)

phase equilibrium determined by the Gibbs conditions

- * **energy minimization (EM)** (surface and Coulomb included in EM)

phase equilibrium determined by energy minimization

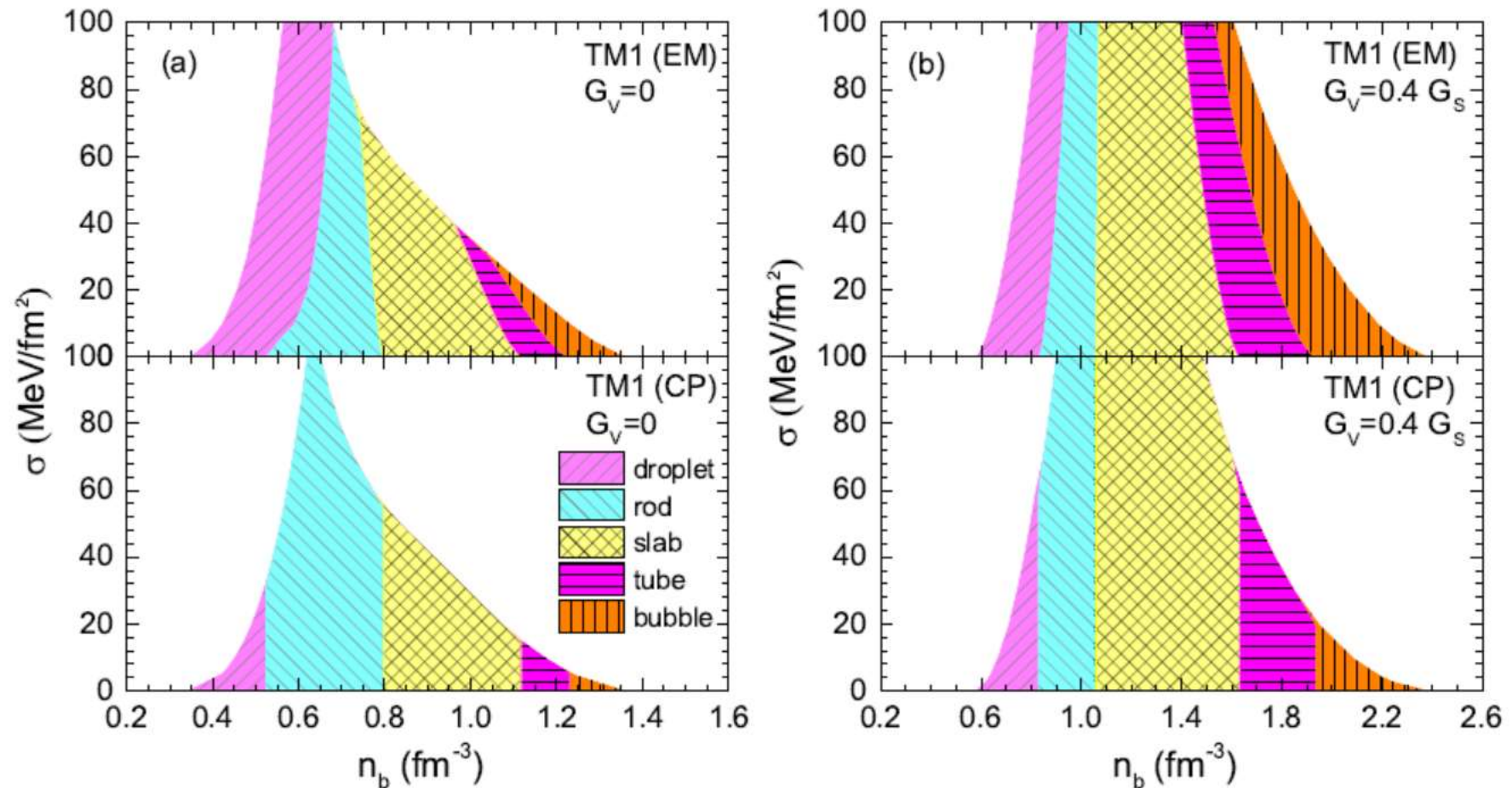
Hadron-quark pasta phases



energy densities for pasta phases

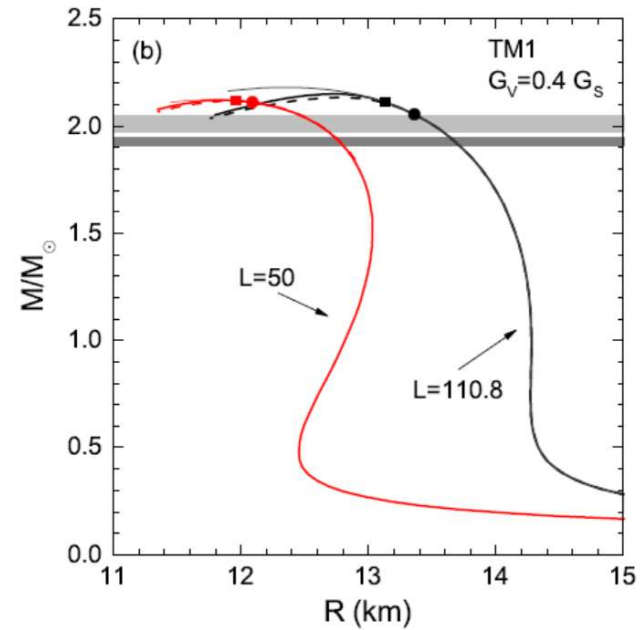
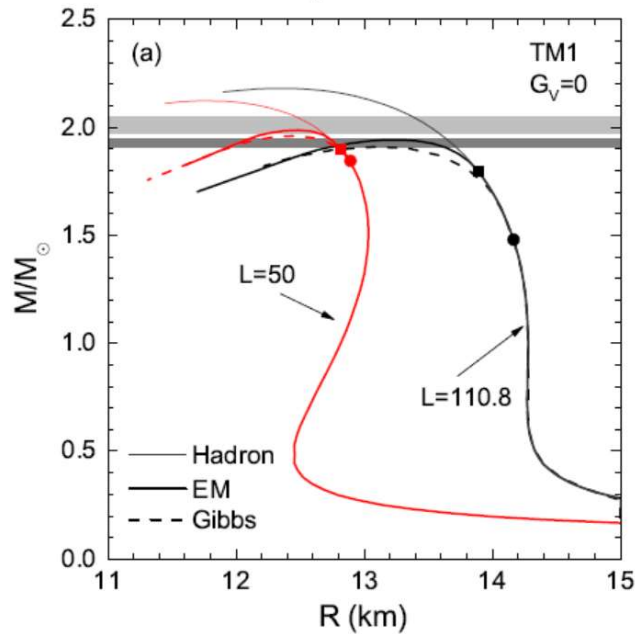
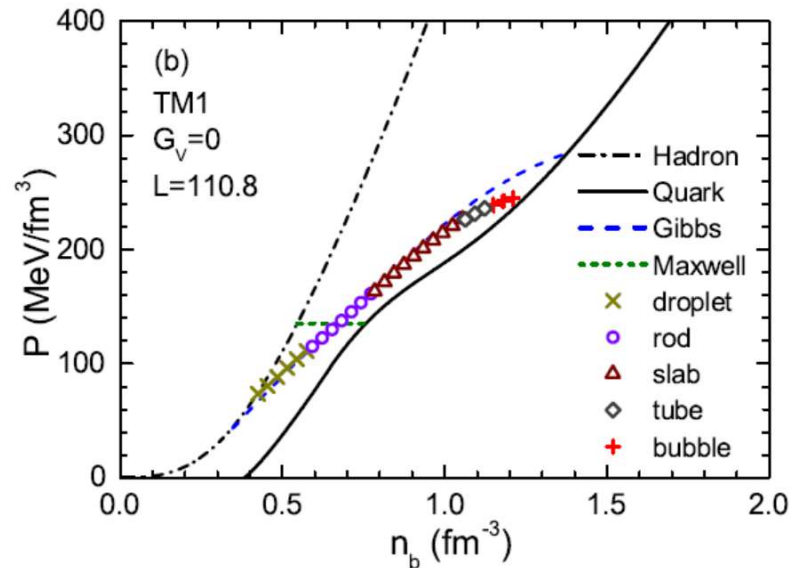
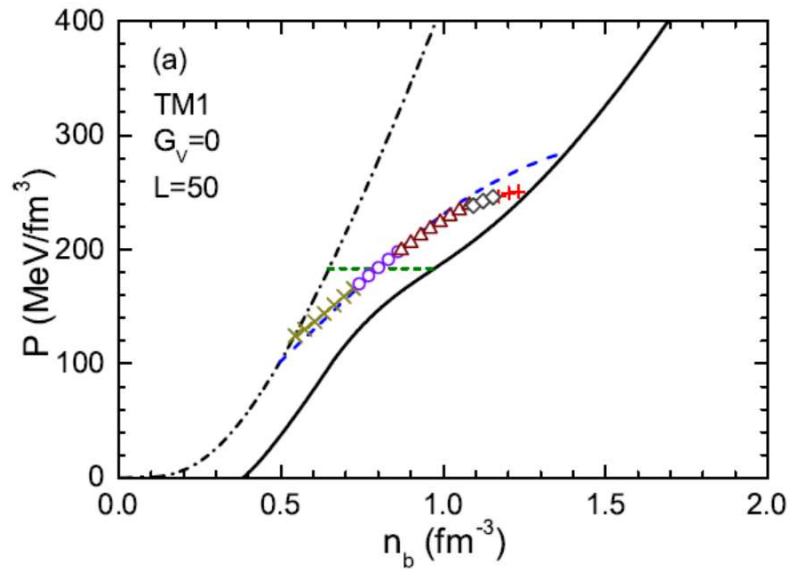
X. H. Wu, H. Shen, Phys. Rev. C 99, 065802 (2019)

Hadron-quark pasta phases



density ranges of pasta phases depend on σ













EOS with quarks




New EOS table for supernovae

http://my.nankai.edu.cn/wlxy/sh_en/list.htm

Homepage of EOS tables

version	model	main table	table for $T=0$	table for $Y_p=0$
EOS1	TM1 (1998) n	 eos1.tab.gz	 eos1.t00.gz	 eos1.yp0.gz
EOS2	TM1 (2011) n	 eos2.tab.zip	 eos2.t00.zip	 eos2.yp0.zip
EOS3	TM1 (2011) n+Lambda	 eos3.tab.zip	 eos3.t00.zip	 eos3.yp0.zip
EOS4	TM1e (2019) n	 eos4.tab.zip	 eos4.t00.zip	 eos4.yp0.zip

 **EOS4**

nuclear interaction: extended TM1 model (TM1e) with $L=40$

nonuniform matter: Thomas-Fermi approximation

ranges and grids: the same as EOS2

New EOS table for supernovae

constraints	EOS2 (TM1)	EOS4 (TM1e)
nuclear matter	isoscalar n_0 , E/A , K ✓ $E_{\text{sym}}=36.9$ MeV ✗ $L=110.8$ MeV ✗	same ✓ $E_{\text{sym}}=31.4$ MeV ✓ $L=40$ MeV ✓
finite nuclei	binding energies and radii ✓ E/A (^{208}Pb)= 7.88 MeV ✓ Δr_{np} (^{208}Pb)= 0.16 fm	similar ✓ E/A (^{208}Pb)= 7.88 MeV Δr_{np} (^{208}Pb)= 0.27 fm
neutron star mass	$M_{\text{max}}=2.18 M_{\odot}$ ✓	$M_{\text{max}}=2.12 M_{\odot}$ ✓
radius	$R_{1.4}=14.2$ km ✗	$R_{1.4}=13.1$ km ✓
tidal deformability	$\Lambda_{1.4}=1047$ ✗	$\Lambda_{1.4}=652$ ✓

effects of symmetry energy on: {
 supernova simulation
 neutron star cooling
 binary neutron star merger ...

Summary

- Unified EOS is important for neutron stars
- Pasta phases in the inner crust depend on L
- Hadron-quark pasta phases may exist
- Neutron-star radius is sensitive to L
- New EOS table is available